Effects of glucose concentration on myoblast differentiation, muscle fiber composition and CB1 receptor expression

Presented to the faculty of Lycoming College in partial fulfillment

of the requirements for Departmental Honors in

Biology

By

Kathy Jacobs

Lycoming College

February 20, 2014

Approved by:

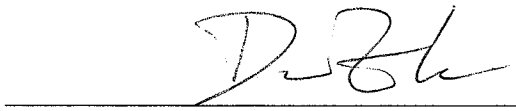

Dr. Dongjiao Zhao, PI

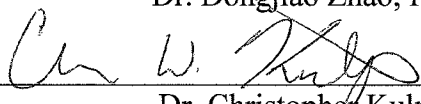

Dr. Christopher Kulp

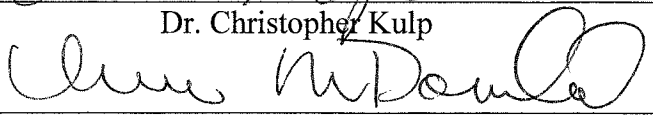

Dr. Chriss McDonald

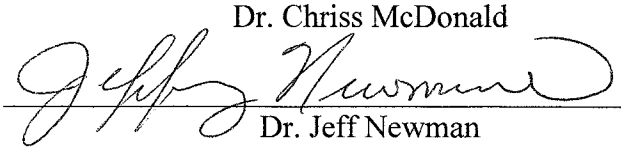

Dr. Jeff Newman

Effects of varying glucose concentrations on myoblast differentiation, muscle fiber composition and CB1 receptor expression

Kathy Jacobs

Honor's Project Thesis

Project Director: Dr. Dongjiao Zhao

Committee: Dr. Christopher Kulp, Dr. Chriss McDonald, Dr. Jeff Newman

Lycoming College

February 6, 2014

Abstract:

Glucose is most important simple sugar for the human body, and changes in extracellular and intracellular glucose concentrations can have a dramatic effect on a cell's morphology and function. Studying these effects is of high importance due to the increasing presence of type II diabetes in the United States' population. In this study, C2C12 cells, muscle myoblasts, were differentiated at various concentrations of glucose (10 mM, 15 mM, and 25 mM) in order to determine how glucose levels affected differentiating muscle stem cells. RNA was isolated after one day of differentiation and after the cells were fully differentiated at day six. RT-qPCR was run to determine how differentiation time and glucose concentration affected gene expression levels. Muscle fiber composition was studied using myosin heavy chain (MHC) primers and the three primers were used to determine the gene expression levels of the cannabinoid 1 receptor (CB1R). Gene expression levels of CB1R and MHCIIx (fast muscle fiber) increased dramatically in the high glucose sample of fully differentiated cells. It can be suggested that altering glucose levels is enough to alter the muscle fiber composition of skeletal muscle cells. Further studies need to be performed to determine if there is a relationship between the increase in CB1R expression and the increase is fast muscle fibers (MHCIIx expression).

Introduction:

Diabetes Mellitus

In individuals with diabetes mellitus, the process in which sugar is taken into the cell and used as an energy source has malfunctioned. As a result, the sugar concentration in the cell is too low, and the sugar concentration in the blood is too high. It is difficult to measure the exact concentration of glucose inside the cells, and as a result, the level of intracellular glucose in diabetic patients needs be confirmed by additional study. High blood glucose levels result in numerous symptoms such as fatigue, frequent infections, and excess urination (American Diabetes Association, 2013).These malfunctions are a result of complications of a hormone in the body called insulin. Insulin allows the cells to utilize the sugar in the bloodstream. Without insulin, sugar cannot enter the cells and as a result, the body is unable to metabolize the sugar into components the cell can use as energy. As a result, as glucose uptake becomes impaired, less glucose is available for the cell to metabolize. Some researchers, however, believe that there are additional effects that cause a lower intracellular concentration than just the impairment in the uptake of glucose (Thorburn, 1990). In diabetes mellitus type 1, the body cannot produce insulin, whereas in diabetes mellitus type 2, the body either cannot make enough insulin to compensate for the high sugar intake or the body stops responding to insulin. All of these changes result in a decrease in sugar available to the cell. Without an adequate energy source, cells begin to lose function. All areas of the body feel the effect of diabetes, but because of its metabolic role, the effects of diabetes on skeletal muscle is of high importance.

Muscle Fibers

Muscles do not entirely consist of one muscle fiber type but a varying combination of seven fiber types including types I, IC, IIC, IIAC, IIA, IIAB, and IIB. Some researchers, however, only focus on the three original types which are type I, IIA, and IIB. These three types each correlate with a different myosin isoforms: MHCI, MHCIIa, and MHCIIx/d(IIb), respectively. This difference allows measurement of the composition of muscle fiber types through qPCR with different MHC primers (Scott et al., 2001). Past studies have shown that muscles do have the ability to change fiber types depending on environmental conditions (Pette and Staron, 1997).

Jing He et al. did not see a change in muscle fiber types in obese and type 2 diabetic patients, but instead, a change in enzyme activity in the muscles. The oxidative enzyme activity decreased and the glycolytic activity increased in obese and diabetic patients, but this change was independent of the muscle fiber type (2001). A study comparing the oxidative and glycolytic pathways in muscles of patients with type 2 diabetes found, similarly, that there was a reduction in oxidative enzyme activity in patients with type 2 diabetes (Oberbach et al., 2006). However, Oberbach et al. hypothesized that this change was most likely due to a decrease in slow oxidative muscle fibers (2006). Researchers have not yet agreed whether the actual muscle fibers are changing or if the enzymes they produce are changing.

The Endocannabinoid System

In recent years, the endocannabinoid system has become a main area of study as a result of its relationship with metabolic regulation. Studies have shown that the endocannabinoid system (ECS) in obese patients is overactive (Zhao et al., 2010). The ECS is made up of the endocannabinoids, such as anandamide (AEA) and 2-arachidonoylglycerol (2-AG), and receptors, including the cannabinoid type 1 (CB1) receptor and cannabinoid type 2 receptor (CB2R) (Scheen, 2007). Patients who are obese and have type 2 diabetes possess a greater degree of insulin resistance and a greater activation of CB1 receptors than individuals without type 2 diabetes (Scheen, 2007). The degree of insulin resistance combined with an overactive ECS has been a source of study over the past decade. Researchers have used this correlation to decrease body weight and, as a result, decrease the prevalence of type 2 diabetes. One way researchers are doing this is by studying an inverse agonist of the CB1 receptor called Rimonabant (Rim). Rim is found to improve insulin sensitivity, increase glucose uptake, and increase oxygen consumption (Kim et al., 2012, Zhao et al., 2010).

The relationship between CB1 receptor activity and obesity is still somewhat unknown. In an attempt to understand this relationship, researchers have studied how the CB1 inverse agonist decreases body weight. Subjects who were under the treatment of a CB1 inverse agonist were shown to have an increase in whole-body energy expenditure and a decrease in food intake. This suggests that an overactive ECS will stimulate CB1 receptors which will cause an increase in appetite and therefore food intake which will result in changes in metabolic pathways (Crespillo et al., 2011).

RT-qPCR

Over the past 10 years, the number of studies that have used Reverse Transcription-Quantitative Polymerase Chain Reaction (RT-qPCR) has grown exponentially (Taylor et al., 2010). As a result of this increase, guidelines have been set to ensure accurate results are being found. If these guidelines are not met, erroneous data could result. The Minimum Information for Publication of Quantitative Real-Time Experiments (MIQE) contains a checklist of 88 items that should be met in order to ensure accurate results (Bustin et al., 2009). The MIQE guidelines incorporate all aspects of studying gene expression, starting with how the tissue sample should be isolated to RT-qPCR validation and data analysis. If these guidelines are not met, erroneous data will result, which has no significance (Lanoix et al., 2012).

The question has been raised as to whether the CB1R is involved in the changing muscle fiber composition. Studying the gene expression levels of CB1R and the composition of muscle fibers at varying glucose levels is the first step in determining if there is a relationship. Later, agonists and antagonists of CB1R can be added to determine whether this has an effect on the muscle fiber composition.

Methods:

***Culturing of C2C12 Cells*.** C2C12 cells were cultured in Dulbecco's Modified Eagle Medium (DMEM, 25 mM glucose) supplemented with10% fetal bovine serum (FBS) and 1% antibiotics (100 units/mL penicillin and 100 ug/mL streptomyosin). On approximately day 7, cells were split and grown until they reached 80-90% confluency.

Differentiation of C2C12 Cells. To initiate differentiation, when cells were 80-90% confluent, differentiation medium was added consisting of 2% horse serum, 1 % antibiotics (100 units/mL penicillin and 100 ug/mL streptomyosin), and varying levels of glucose in DMEM. These levels will be referred to as low (L, 10 mM glucose), medium (M, 15 mM glucose), and high (H, 25 mM glucose).

RNA Isolation using Aurum Total RNA Mini Kit. Cells were removed from plates using trypsin and following standard protocol. RNA was isolated using the Aurum Total RNA Mini Kit (Bio-Rad, Catalog #732-6820). The manufacturer protocol for adherent cell cultures was followed. RNA was isolated 24 hours after differentiation (referred to 1L,1M, and 1H) and when the cells were fully differentiated, 6 days in differentiation medium (referred to as 6L, 6M, 6H).

***Examining the Concentration of RNA isolated*.** After RNA isolation was performed, the concentration was measured using the Qubit® 2.0 Fluorometer. The standard protocol for RNA samples was followed.

***Reverse Transcription of RNA*.** RNA was reverse transcribed into cDNA using the iScript cDNA Synthesis Kit (Bio-Rad, Catalog # 170-8891) following the protocol provided by the

manufacturer. Prior to the reaction, the RNA was denatured at 70˚C for 10 minutes. One microgram total RNA was used in each reaction, so depending on the starting concentration of the RNA sample, the volume of RNA in the reaction differed. The total reaction volume for each sample was 20 µl.

***Designing Primers*.** The myosin heavy chain primers (MHCIb, IIa, IIb, and IIx) and 18S rRNA were found in past studies using mice. The MHC primers were from Girgenrath's work and 18S rRNA, CB1_1 and CB1_3 were from Zhao's work (2004, 2010). The Cnr1 primer was based off of Crespillo's (2011) study that used rats as the subjects. The forward and reverse Cnr1 primer was compared to the Cnr1 gene in mice using NCBI and a base pair in each the forward and reverse primer was altered. The MYH7_1 and MYH7_3 primers were designed using NCBI's Primer-BLAST software (Table 1).

	Forward (5'--> 3')	Reverse (5'--> 3')	Annealing temp, used ˚C
18S rRNA	CGGCTACCACATCCAAGGAA	GCTGGAATTACCGCGGCT	55
Cnr1	AGACCTCCTCTACGTGGGCTCA	AGGACAGCGATGGCCAGCTGCTG	55
MHCIb	CCTGGAGAAACCTGCCAAGTATGATGACA	CTGCTTCCACCTAAAGGGCTG	55
MHCIIa	AAGCGAAGAGTAAGGCTGTC	CTTGCAAAGGAACTTGGGCTC	50
MHCIIx	GAAGAGTGATTGATCCAAGTG	TATCTCCCAAAGTTATGAGTACA	47
MHCIIb	GAAGAGCCGAGAGGTTCACAC	CAGGACAGTGACAAAGAACGTC	50
CB1_1	GAATGATTGGGCTAAGG	AAAAAGGGGTACTGCCCT	46
CB1_3	CCTTGCAGATACAACCTT	TGCCATGTCTCCTTTGATA	46
MYH7_1	AGAATTCTCCTGCTGTTTCCTT	CCGTCTTGCCATTCTCCGT	55
MYH7_4	ATCTTGTCGAACTTGGGTGGG	GCTGTTTCCTTACTTGCTACCC	55

Table 1. Forward and reverse primer sequences from Girgenrath's (2004) and Zhao's (2010) study, the Cnr1 primer based off of Crespillo's (2011) study, and the MYH7 primers designed using NCBI's Primer-BLAST software.

RT-qPCR. 10 µl of SYBR green (Bio-Rad, 172-5264),1 µl of forward primer (20 µM) , 1 µl of reverse primer (20 µM), and varying amounts of cDNA template (1 µl, 2 µl, or 4 µl) and nuclease free water to make a final volume of 20 µl were added to an eight-tube strip of 0.2 ml tubes. RT-qPCR reactions were performed in triplets. All three volumes of complementary DNA (1 µl, 2 µl, or 4 µl) were used to form the standard curve, but for all the other samples, 2 µl of cDNA was used. Tubes were centrifuged and placed in the CFX96 Touch Real-Time PCR Detection System and the run on table three was programed.

RT-qPCR run (with melting curve)
1. 50˚C 2 min, 1 cycle
2. 95˚C 10 min, 1 cycle
3. 95˚C 15 sec → Annealing temperature 30 sec → 72˚C 30 sec, 40 cycles
4. 72˚C 10 min, 1 cycle
5. Melting Curve: 65˚C 5 sec →95˚C, •0.5˚C/cycle
6. 4˚C hold

Table 2*.* Run used for RT-qPCR. Step 5 is an optional melting curve.

Post RT-qPCR procedures*.* After RT-qPCR was performed, the PCR product was then run on an agarose gel to determine if the product produced was the correct length.

Data Analysis of RT-qPCR product*.* The RT-qPCR data was analyzed using Bio-Rad CFX Manager. All measurements were taken at 100 Relative Fluorescent Units (RFU).

- *For CQ analysis*, the CQ's of the samples were compared at 100 RFU. The higher the CQ value, the lower the gene expression.

- *For SQ analysis*, a standard curve was first formed using the Day 6 High Glucose samples (6H). The varying levels of cDNA (1 µl, 2 µl, and 4 µl) of the 6H samples were

graphed and a standard curve was formed (see Table 4). The SQ value for all the other samples was then calculated based off of the standard curve formed from the 6H samples.

***Table 3*. Forming a Standard Curve**

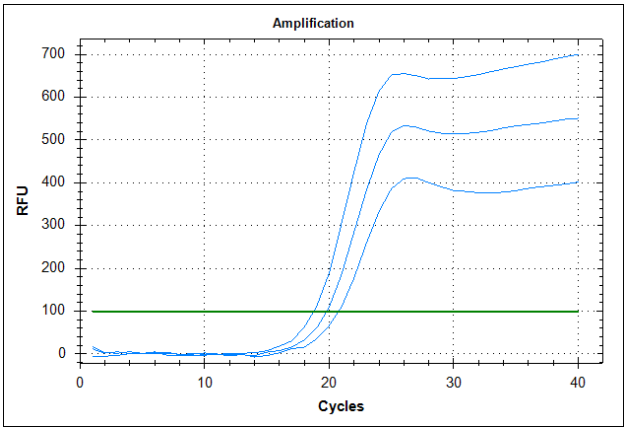

1. Identify the 1 µl, 2 µl, and 4 µl cDNA samples.

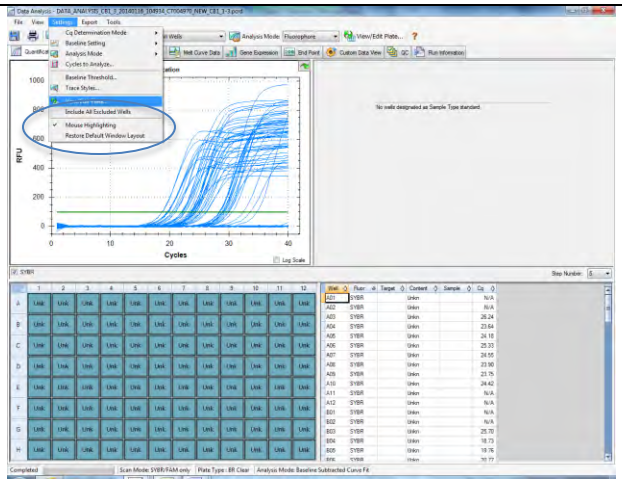

2. Click View/Edit plate under Settings.

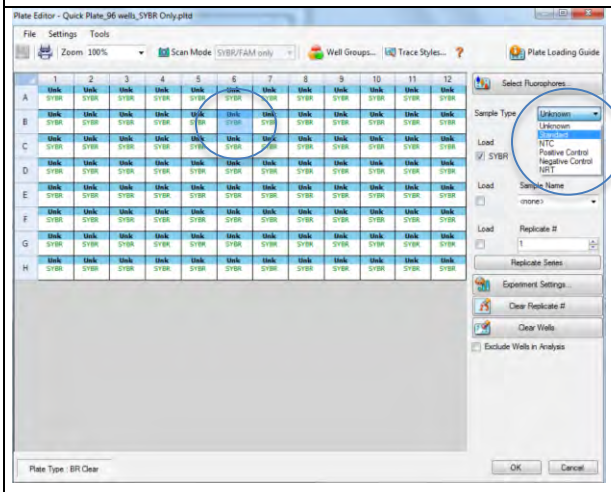

3. Click on the well where the 1 µl sample is located. Once highlighted, under sample type, choose Standard.

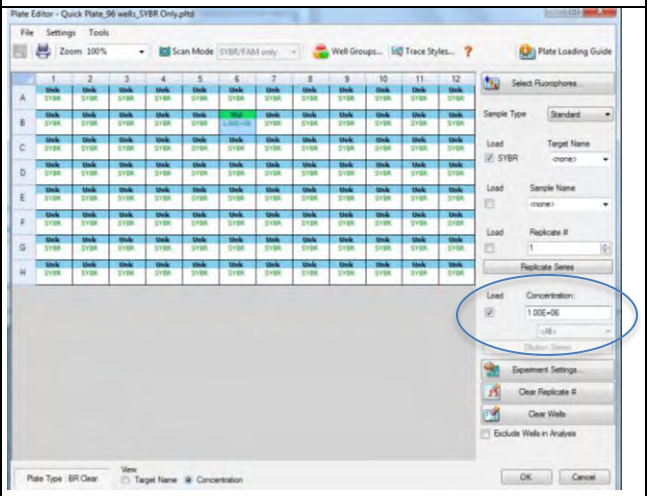

4. Check the Load box and in the concentration box, type 1.00E+06. Repeat steps 3 and 4 with the 2 µl and 4 µl samples, changing the concentration to 2.00E+06 and 4.00E+06 respectively.

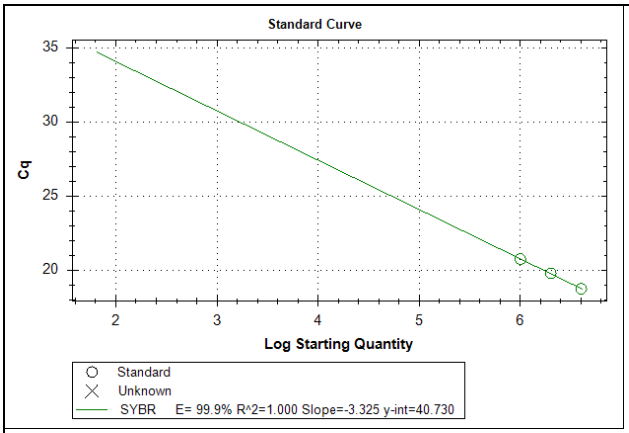

5. A standard curve will automatically form.

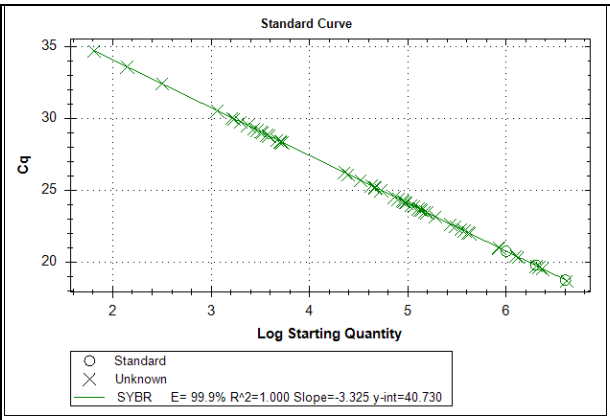

6. Based off of the standard curve, all other concentrations will be calculated.

Once the SQ value was found for a given sample, the SQ value of that sample was divided by the SQ of the housekeeping gene, 18S rRNA, for that specific sample. For example, the SQ value of 1L using the MHCIIx primer was divided by the SQ value of 1L using the 18S rRNA primer. This was performed in order to account for differences in cDNA levels of the samples.

Results:

Culturing of Cells:

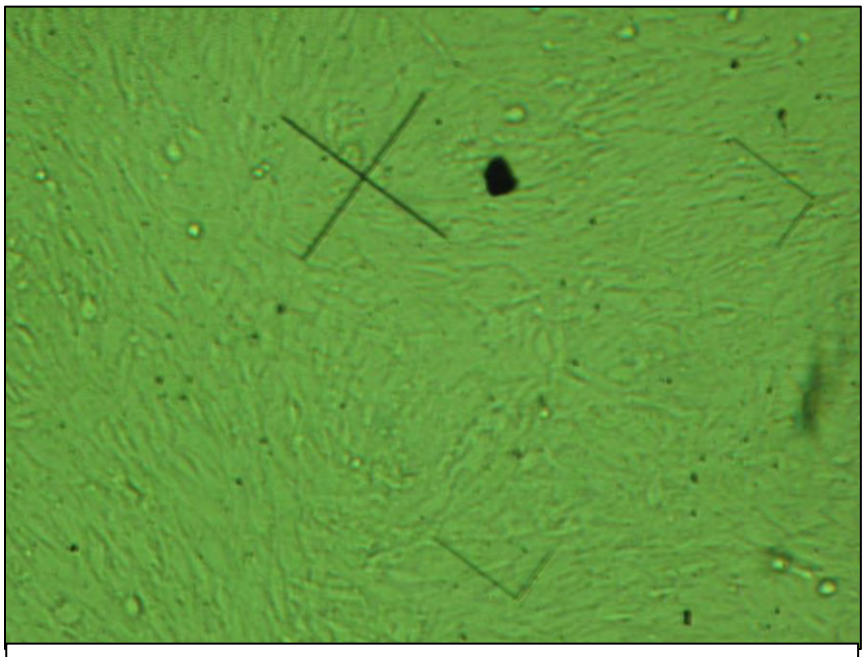

Figure 1. Undifferentiated C2C12 cells grown in 10% FBS and DMEM (25 mM glucose) at 100x magnification.

Figure 1 shows a microscope image of undifferentiated C2C12 cells that are about 90% confluent.

Cell Differentiation:

Cells After Differentiation (2% Horse Serum)

	Day 1 (24 hours after differentiation)	Day 3	Day 6
Low (10 mM)	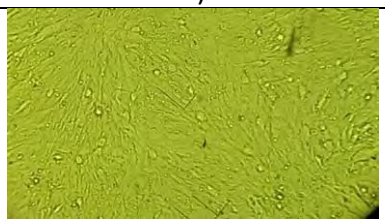	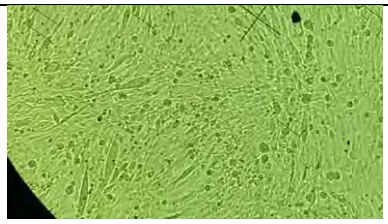	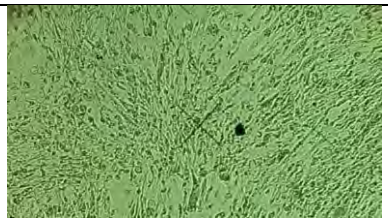
Medium (15 mM)	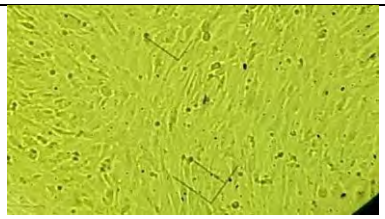	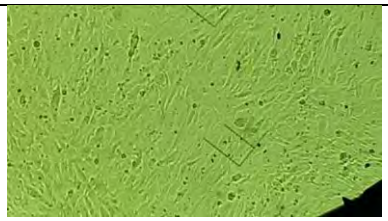	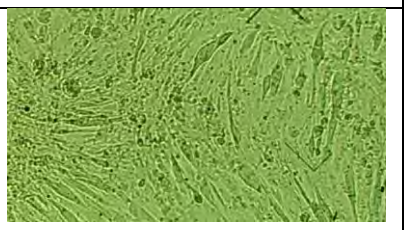
High (25 mM)	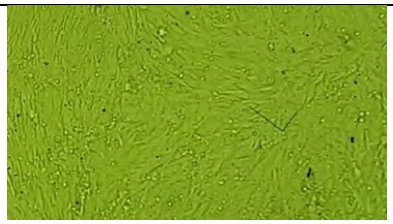	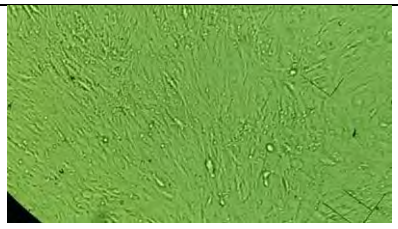	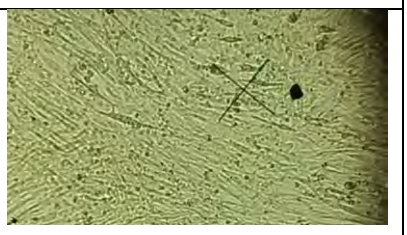

Figure 2. Day 1,3, and 6 differentiated C2C12 cells grown in 2% horse serum and DMEM with varying levels of glucose (10 mM, 15 mM, and 25 mM) at 100x magnification.

Figure 2 shows the progression of differentiation over the course of six days. Changes in cell morphology could be seen as early as day one. As differentiation time increased, the cells became larger and more fiber-like. Cell death was more evident with the low glucose sample at day six.

RNA Isolation:

The RNA isolated from the medium glucose sample at day six was not concentrated enough to continue to the next step of reverse transcription. As a result, the remaining samples analyzed using RT-qPCR were 1L, 1M, 1H, 6L and 6H.

RT-qPCR:

Housekeeping Gene: 18S rRNA

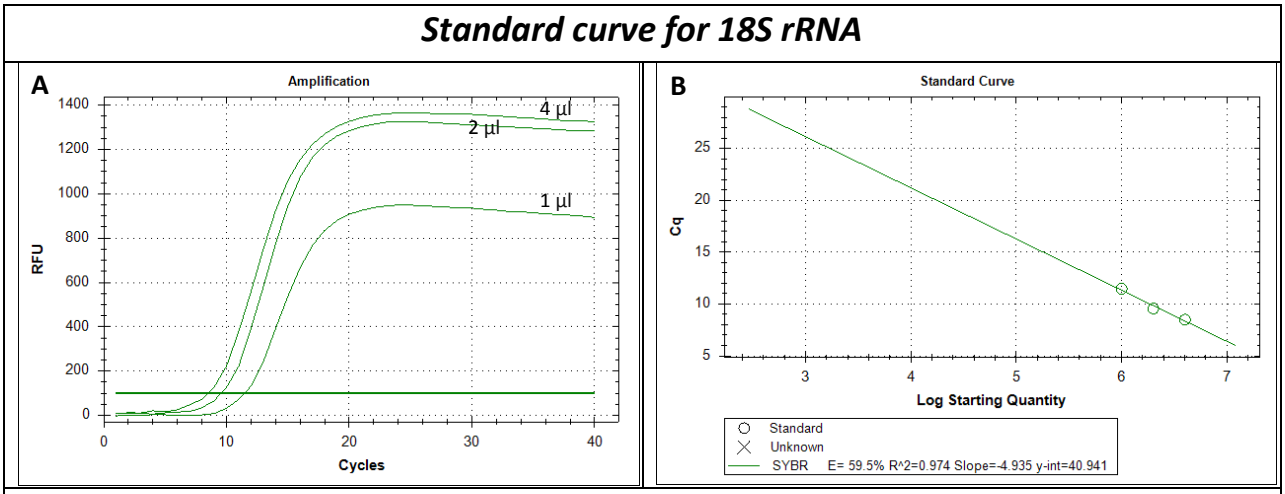

Figure 3. A is a RT-qPCR amplification graph for the 18S rRNA primer indicating the relative fluorescence units (RFU) over 40 cycles. B is a standard curve graph with the points indicating the 1 µl, 2 µl, and 4 µl samples.

Figure 3A shows that as concentration of cDNA increased, the cycle number (Cq) it took to reach a specific threshold (in this case 100 RFU) decreased. Figure 3B shows the plotted three points (1 µl, 2 µl, and 4 µl). All other samples were given a concentration (SQ) based on their Cq value at 100 RFU and the standard curve produced in Figure 3B.

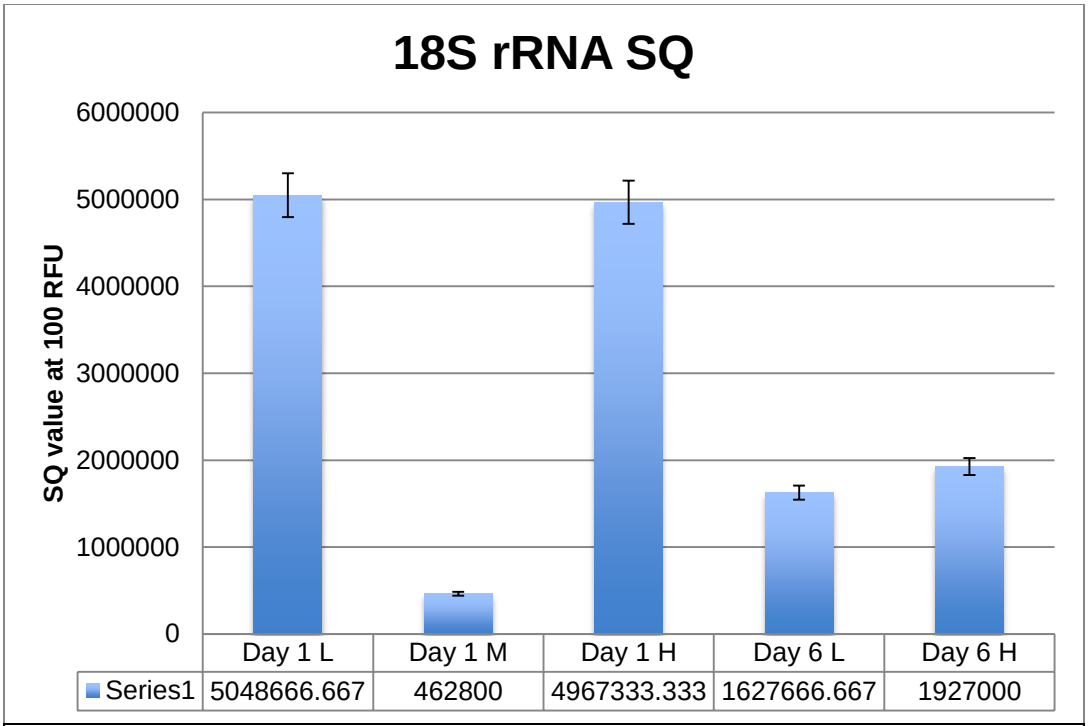

Figure 4. SQ value (y-axis) of 18S rRNA for the five samples (x-axis).

The concentration of 18S rRNA, the housekeeping gene is highest in the low and high glucose samples on day one, and both had very similar SQ values. Both low and high glucose concentrations at day six had very similar SQ values, but these values were much less than the day one samples. Day one medium glucose concentration showed a very low concentration of 18S rRNA.

CB$_1$R Primers

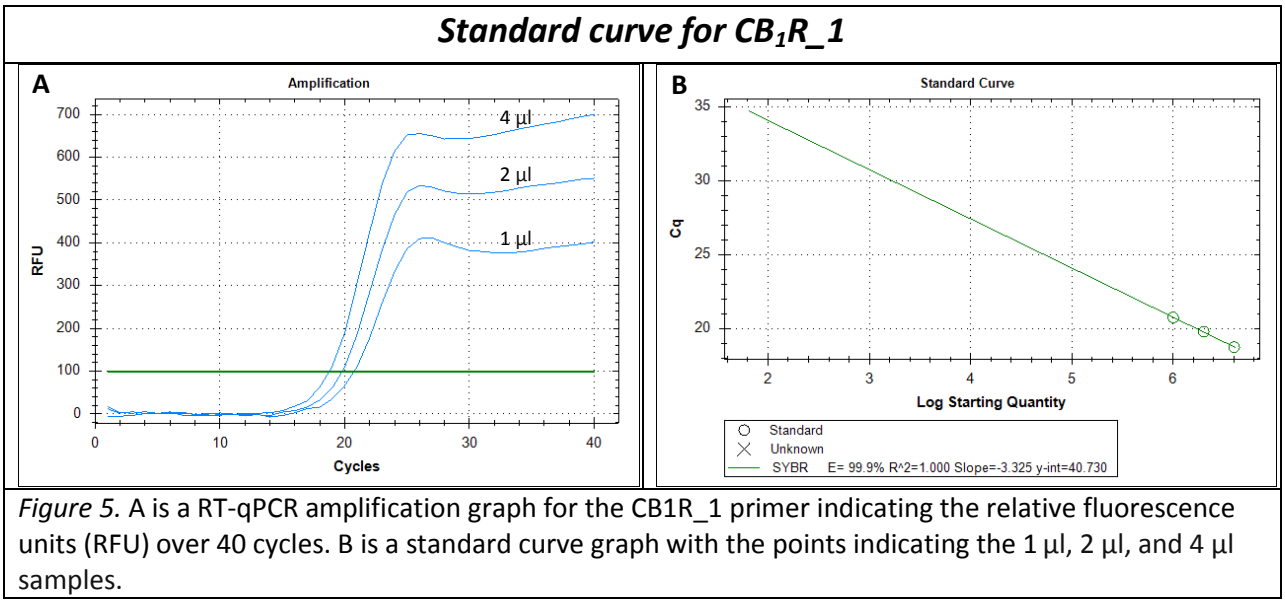

Figure 5. A is a RT-qPCR amplification graph for the CB1R_1 primer indicating the relative fluorescence units (RFU) over 40 cycles. B is a standard curve graph with the points indicating the 1 µl, 2 µl, and 4 µl samples.

Figure 5A shows that as concentration of cDNA increased, the cycle number (Cq) it took to reach a specific threshold (in this case 100 RFU) decreased. Figure 5B shows the plotted three points (1 µl, 2 µl, and 4 µl). All other samples were given a concentration (SQ) based on their Cq value at 100 RFU and the standard curve produced in Figure 5B.

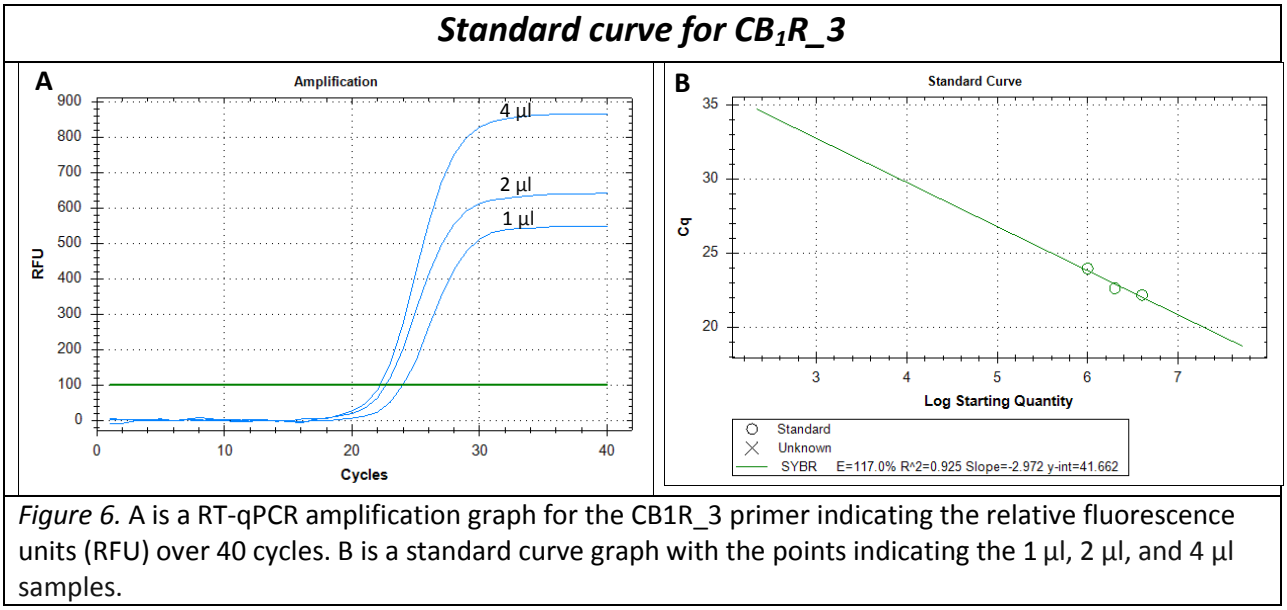

Figure 6. A is a RT-qPCR amplification graph for the CB1R_3 primer indicating the relative fluorescence units (RFU) over 40 cycles. B is a standard curve graph with the points indicating the 1 µl, 2 µl, and 4 µl samples.

Figure 6A shows that as concentration of cDNA increased, the cycle number (Cq) it took to reach a specific threshold (in this case 100 RFU) decreased. Figure 6B shows the plotted three points (1 µl, 2 µl, and 4 µl). All other samples were given a concentration (SQ) based on their Cq value at 100 RFU and the standard curve produced in Figure 6B.

**The 2 µl sample for the standard curve of the Cnr1 primer had a lower Cq value than the 4 µl sample, and as a result, a standard curve could not be formed. Because of the lack of a standard curve, the Cnr1 data was not analyzed further.

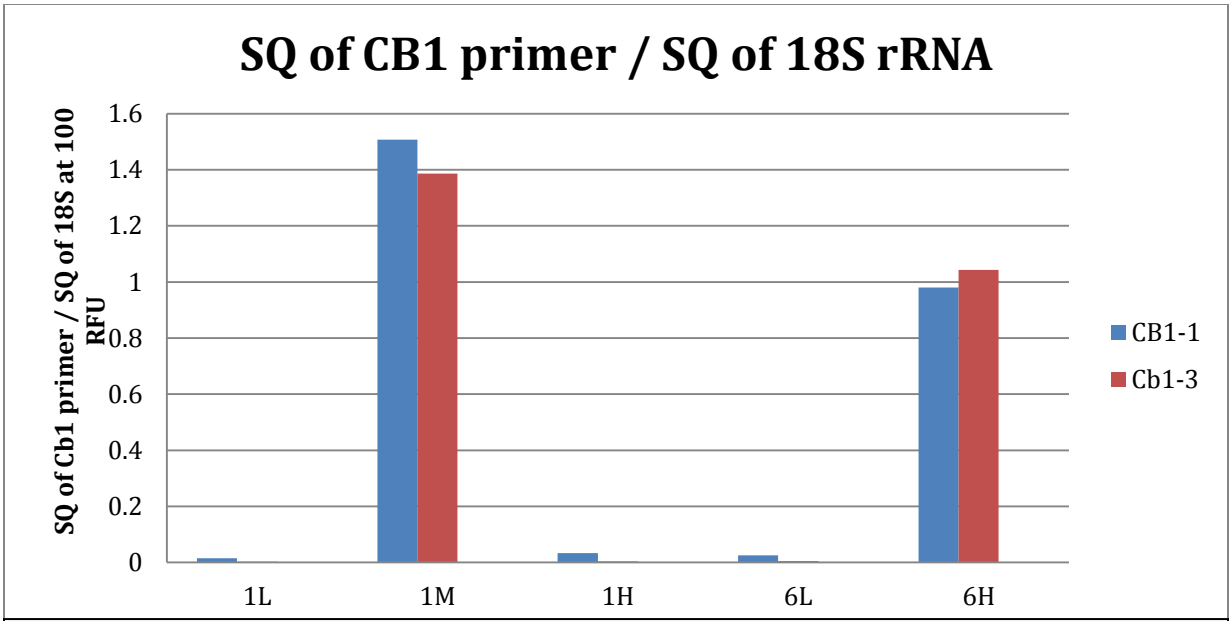

Figure 7. Concentration of RT-qCPR product using CB1_1 (blue) and CB1_3 (red) primers for the five samples (x-axis).

In Figure 7, the concentration of RT-qPCR product for both CB1_1 and CB1_3 primers were graphed in order to see if they showed the same gene expression levels. Both primers showed the same gene expression levels, peaking at 1M and 6H.

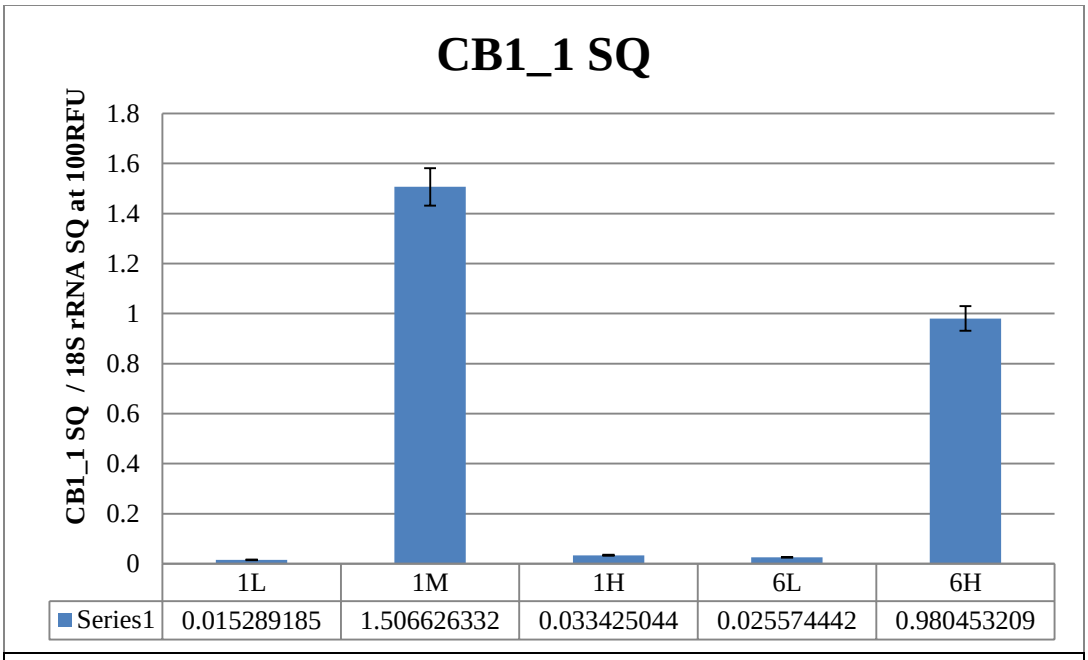

Figure 8. Gene expression levels of CB1R using the CB1_1 primer.

Figure 8 shows that the samples that showed the most gene expression of CB1R were 1M and 6H.

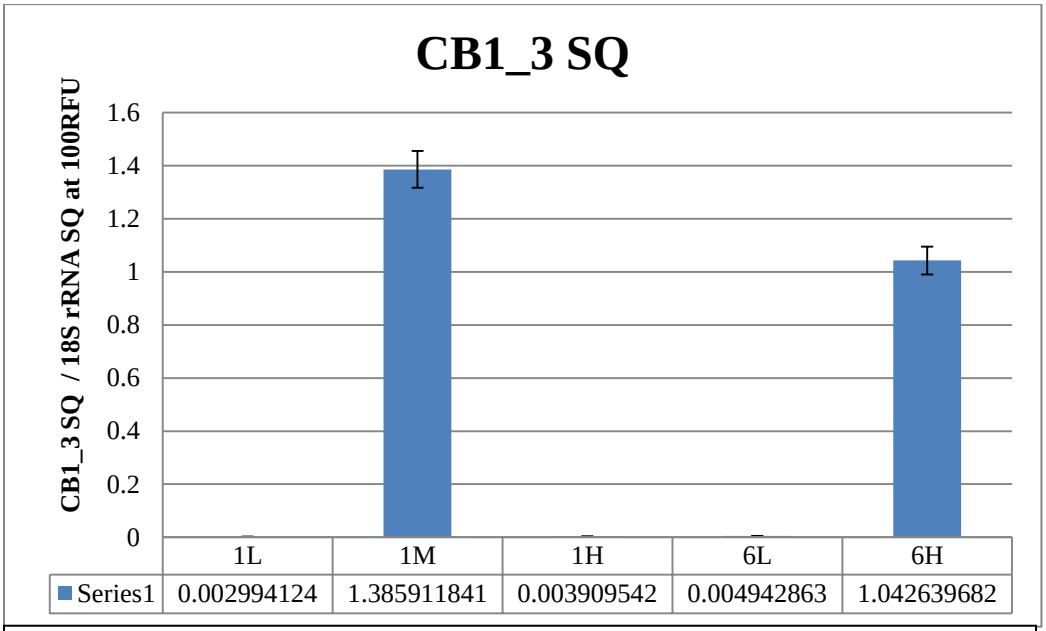

Figure 9. Gene expression levels of CB1R using the CB1_3 primer.

Similar to Figure 8, in Figure 9 the gene expression of CB1R was the highest in the 1M and 6H samples.

MHCIIx Primer

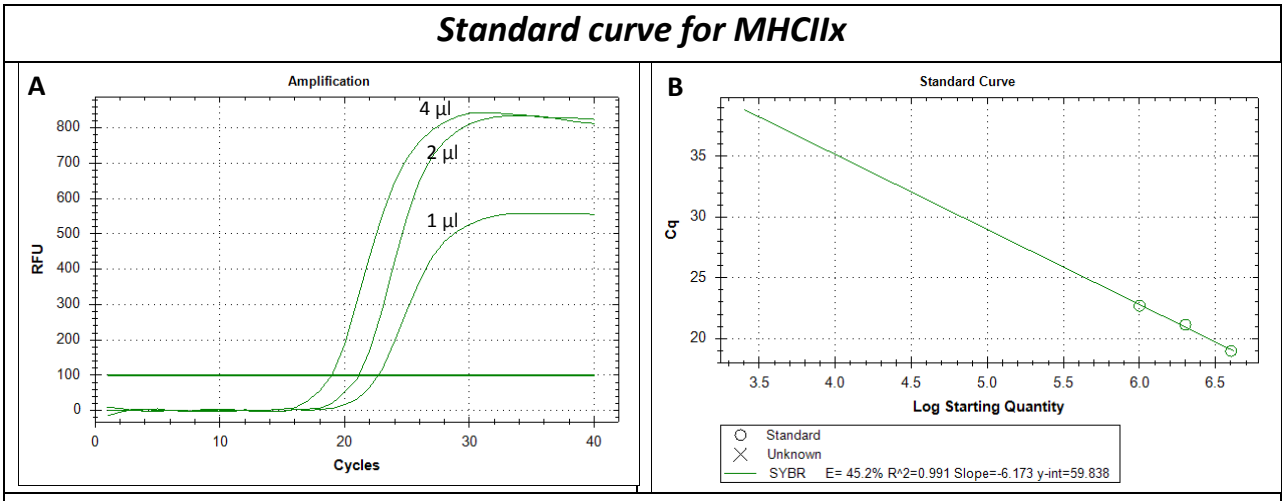

Figure 10. A is a RT-qPCR amplification graph for the MHCIIx primer indicating the relative fluorescence units (RFU) over 40 cycles. B is a standard curve graph with the points indicating the 1 µl, 2 µl, and 4 µl samples.

Figure 10A shows that as concentration of cDNA increased, the cycle number (Cq) it took to reach a specific threshold (in this case 100 RFU) decreased. Figure 10B shows the plotted three points (1 µl, 2 µl, and 4 µl). All other samples were given a concentration (SQ) based on their Cq value at 100 RFU and the standard curve produced in Figure 10B.

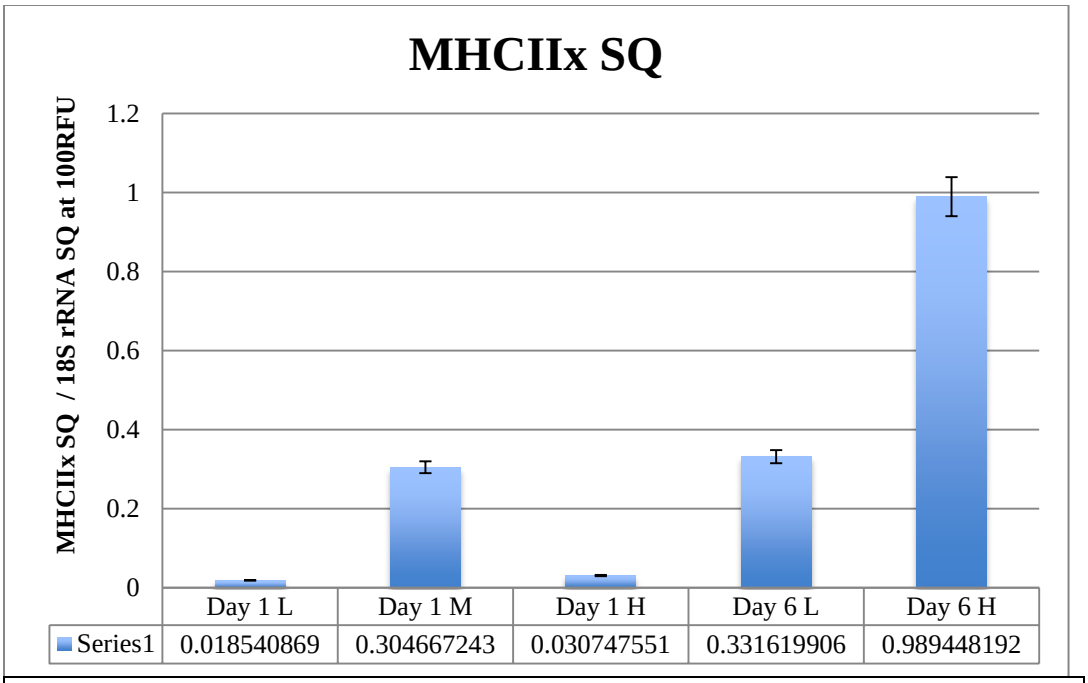

Figure 11. Gene expression levels of MHCIIx (fast muscle fibers)

Figure 11 shows that both 1L and 1H had very low gene expression of MHCIIx, while IM and 6L had moderate gene expression of MHCIIx. 6H had the greatest gene expression levels of MHCIIx.

Gels of RT-qPCR Product

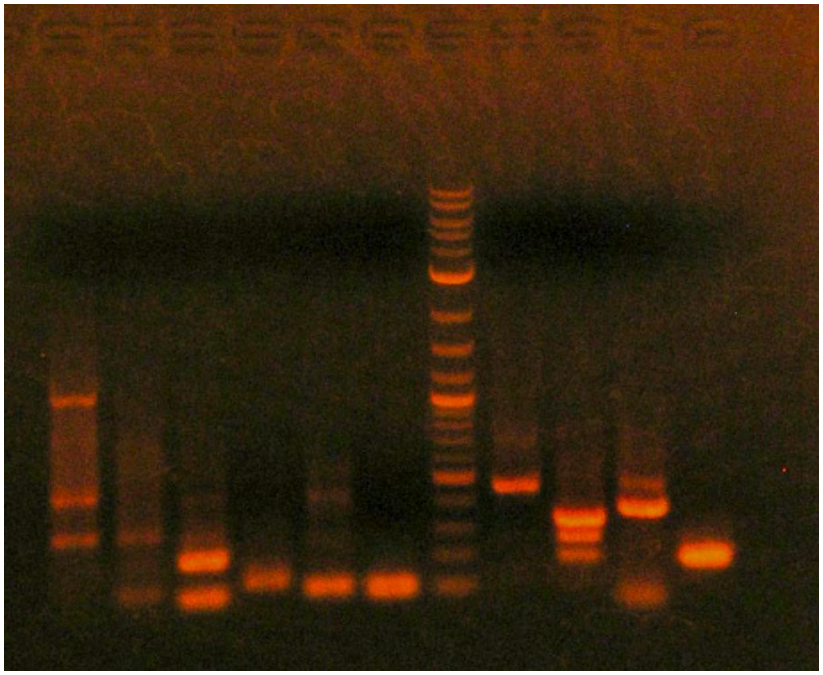

Figure 12. Agarose gel of RT-qPCR product

Well 1	Cnr1
Well 2	CB1_1
Well 3	CB1_3
Well 4	MHCIIa
Well 5	MHCIIb
Well 6	MHCIIx
Well 7	2 log ladder
Well 8	MHCIB
Well 9	MYH7_1
Well 10	MYH7_4
Well 11	18S rRNA

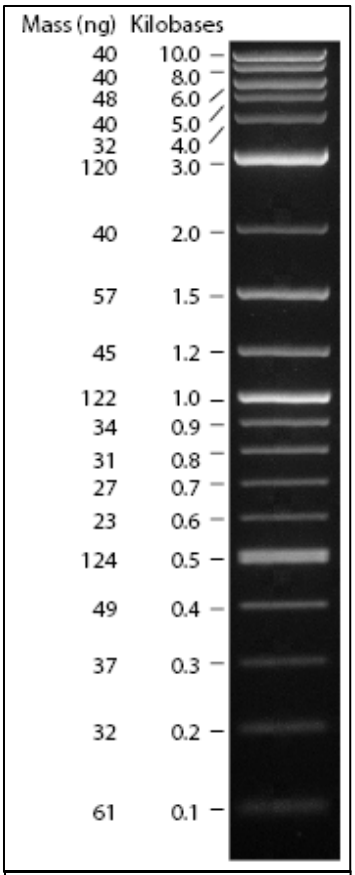

Figure 13. Labeled 2 log ladder that was used in Well 7 on Figure 12.

Figure 12 shows that the RT-qPCR product for all three CB1R primers produced several different bands from 100 to 500 base pairs in length. MHCIIa produced one distinct band at 150 bp. MHCIIb and MHCIIx produced heavy bands at approximately 100 bp. MHCIB had one distinct band at 500 bp. MYH7_1 and MYH7_4 had a strong band between 300-400 bp but also had several weaker bands. The RT-qPCR product of 18S rRNA was seen at about 200 bp with one strong band.

Discussion:

A change in nutrient availability to any cell can have a drastic effect on how the cell operates. Some genes are expressed more, while others are expressed less due to changes in the levels of nutrients available to the cell. Changes in levels of glucose can alter a variety of functions inside the cell. Due to the metabolic properties of skeletal muscle cells, changes in glucose levels change both the composition of the muscle fiber and the expression levels of several genes including the CB1 receptor.

Undifferentiated C2C12 cells are much smaller than differentiated C2C12 cells (Figure 1). As the C2C12 cells differentiated, they became larger and more fiber like. Along with cell growth, there was also cell death. Once the cells were fully differentiated at Day 6, the effects of the low glucose levels could be seen (Figure 2). Although many of the cells were still alive and differentiated in the 6L sample, the low glucose levels prevented the cells from growing and replicating optimally. A 10mM glucose concentration does not seem to be efficient enough to keep C2C12 cells alive for a prolonged period of time. Compared to the other two samples, the cells in the 6M (15 mM glucose) sample showed the greatest degree of differentiation. A large degree of cell differentiation was also seen in the 6H (25mM glucose) sample.

The 18S ribosomal RNA gene (18S rRNA), was used as the reference gene for the RT-qPCR. Suresh Kuchipudi and collogues found that 18S rRNA was the most stable reference gene, when compared to other commonly used housekeeping genes such as beta-actin and glyceraldehyde-3-phosphate dehydrogenase (2012). The cells Kuchipudi used were infected with the influenza virus. However, other experiments have been performed on healthy cells and all lead to the same conclusion. 18S rRNA is a minimally regulated housekeeping gene and

is very reliable as a reference gene in RT-qPCR (Selvey et al., 2001). Environmental conditions should not alter 18S rRNA expression greatly. The much lower concentration of 18S rRNA observed in the 1M sample is concerning (Figure 4). Both the 1L and 1H gene expression levels were very similar. The 6L and 6H samples were also very similar. The day one samples, however, showed a much greater gene expression of 18S rRNA than the day six samples. This difference may have been because the early days of differentiation required more protein production and thus more rRNA production. This, however, does not explain why the 1M sample was so low. Before analyzing the 1M sample, another RT-qPCR should be run with the 1M sample and the 18S rRNA primer. The 18S rRNA SQ value influences all the other samples because the SQ value of every primer is divided by the 18S rRNA SQ value for that specific sample. As a result, a low SQ value as observed in the 1M sample inflated all the other results for the 1M sample. For this reason, the results for the 1M sample will not be analyzed further in this paper.

Three primers were used to study the CB1 receptor: Cnr1, CB1R_1, and CB1R_3. All three primers showed the same pattern of CB1R gene expression (Figure 7 and 19), peaking at 6H. However, all three primers also showed more than one band in the gel of the RT-qPCR product, indicating that multiple products were formed in the RT-qPCR reaction (Figure 12). The melting peaks also all indicate multiple products, due to the bumps in the peak, or in the case of the primer CB1_3, multiple peaks (Figures 15, 16, 17). As a result, a more efficient primer for CB1R should be considered for future studies. However, because all of the primers showed the same pattern of gene expression for the different samples, it was concluded that these primers were still likely producing the proper RT-qPCR product.

The 2 µl samples using the Cnr1 primer had lower Cq values than the 4 µl samples, and as a result, a standard curve could not be formed for the Cnr1 primer. Without a standard curve, the SQ values could not be calculated, and the Cnr1 primer could not be further analyzed. A standard curve was formed from the data using the CB1_1 and CB1_3 primers (Figure 5 and 6). Both primers showed a significant increase in CB1R expression in the 6H sample compared to all other samples (Figure 8 and 9). This increase was not seen, however, in the 1H sample, indicating that it was not simply the high glucose that caused this change but also how long the sample was subjected to the differentiation medium. High glucose coupled with six days of differentiation medium caused the cells to express more CB1R.

The MHCIIx primer indicated how much fast muscle fiber the sample was composed of. Both the 1L and the 1H samples showed low gene expression levels for MHCIIx, while the 6L and 6H showed much greater gene expression levels (Figure 11). As seen in the CB1R expression levels, the 6H sample showed the greatest degree of gene expression. As both differentiation time increased and as glucose concentration increased, the expression of fast muscle fibers increased. Fast muscle fibers are anaerobic and glycolytic which means they produce all of their energy without oxygen and only though glycolysis. Slow muscle fibers are aerobic and oxidative which means they need oxygen in order to make energy, and this energy is made through oxidative phosphorylation. The levels of oxygen remained constant in this experiment. However, the glucose level changed. In the 6H sample, there was a greater level of glucose than the 6L sample. Since the 6H sample had such a large amount of glucose available, it may have been more efficient for the cells to go through just glycolysis instead of oxidative phosphorylation. The 6L sample, however, had a significantly lower concentration of glucose,

and therefore it may have been more efficient for the cells to go through oxidative phosphorylation.

Data for MHCIIa, MHCIIb, MHCIb, MYH7_1, and MYH7_4 was omitted from this paper because a standard curve could not be formed from the data. For MHCIIb and MHCIb, the three different concentrations (1 µl, 2 µl, and 4 µl) of cDNA all had roughly the same Cq values at 100 RFU. For MHCIIa, MYH7_1, and MYH7_4, the different concentrations did not have a linear relationship. As a result, a standard curve could not be formed and SQ concentrations could not be determined for these samples. In the future to prevent this from happening again, the standard curve should be composed of more than three points and the differences in concentrations of cDNA for the standard curve should be more significant. For example, there could be a ten-fold difference in cDNA concentration, instead of the four-fold that was done in this experiment. Also, instead of using one of the samples to generate the standard curve, it may be more reliable to use a target template that is similar to the experimental sample (Life Technologies).

The concentration of insulin was not altered in this study. In order to mimic diabetes in the best possible way in the future, the cell culture should contain various levels of insulin in addition to the various levels of glucose. Type II diabetic patients are both hyperglycemic and have some level of insulin resistance (Brownlee, 2001). This study has accounted for the hyperglycemia but has not accounted for the insulin resistance. As a result, the experimental conditions are more similar to pre-type II diabetic patients or obese patients, where the glucose levels are high but there is not yet a problem with insulin.

With the data collected and studied in this experiment, it can be suggested that an increase in glucose concentration in differentiating C2C12 cells causes an increase in both CB1R and MHCIIx (fast muscle fiber). If this is truly what is happening, as was seen in this data, the next step is to determine if there is a relationship between the changing muscle fiber and the level of CB1R. In a future experiment, the CB1R can be manipulated using agonists and antagonists. If the agonists and antagonists alter the MHCIIx gene expression, there may be a relationship between the muscle fiber composition and the expression of CB1R.

Supplemental Data:

Melting Curves

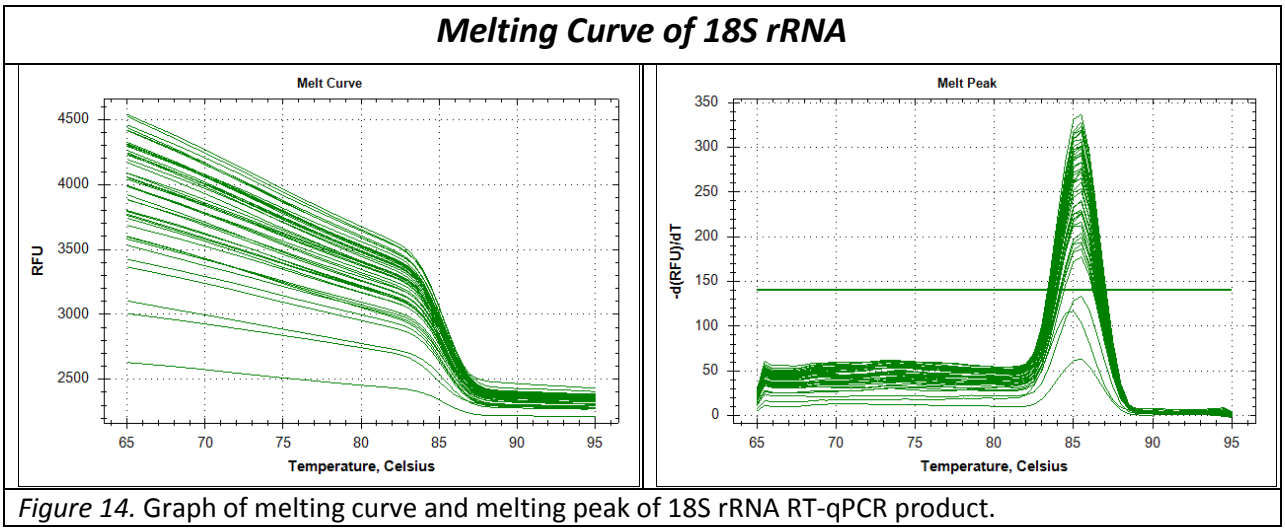

Figure 14. Graph of melting curve and melting peak of 18S rRNA RT-qPCR product.

Figure 14 shows that all the RT-qPCR product using the 18S rRNA primer had the same melting point at about 85°C.

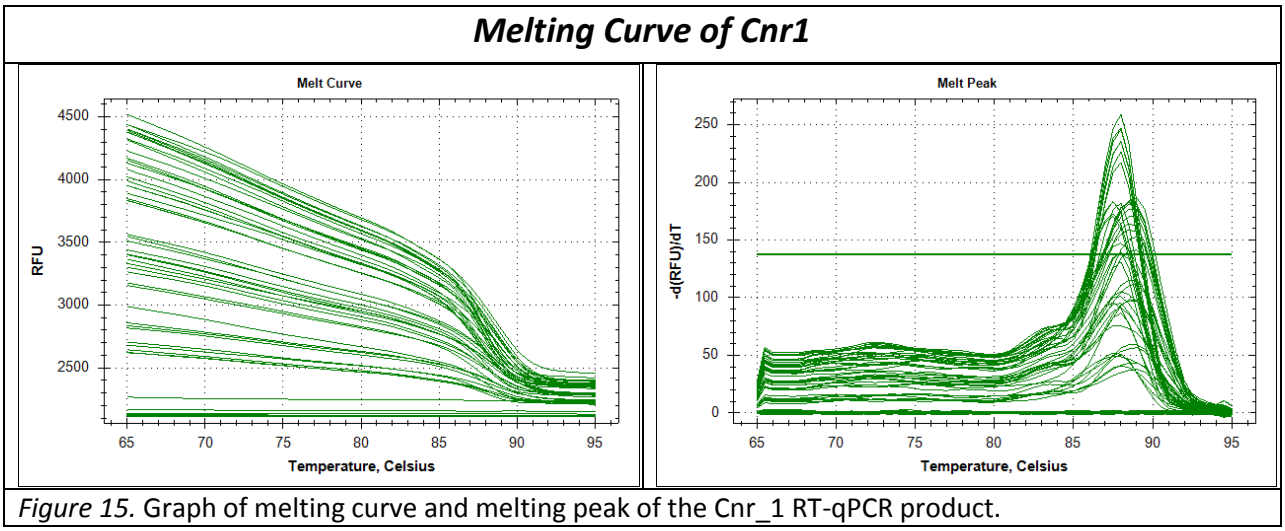

Figure 15. Graph of melting curve and melting peak of the Cnr_1 RT-qPCR product.

Figure 15 shows one prominent peak at approximately at 87°C, but also shows less prominent peaks at 85°C and 89°C.

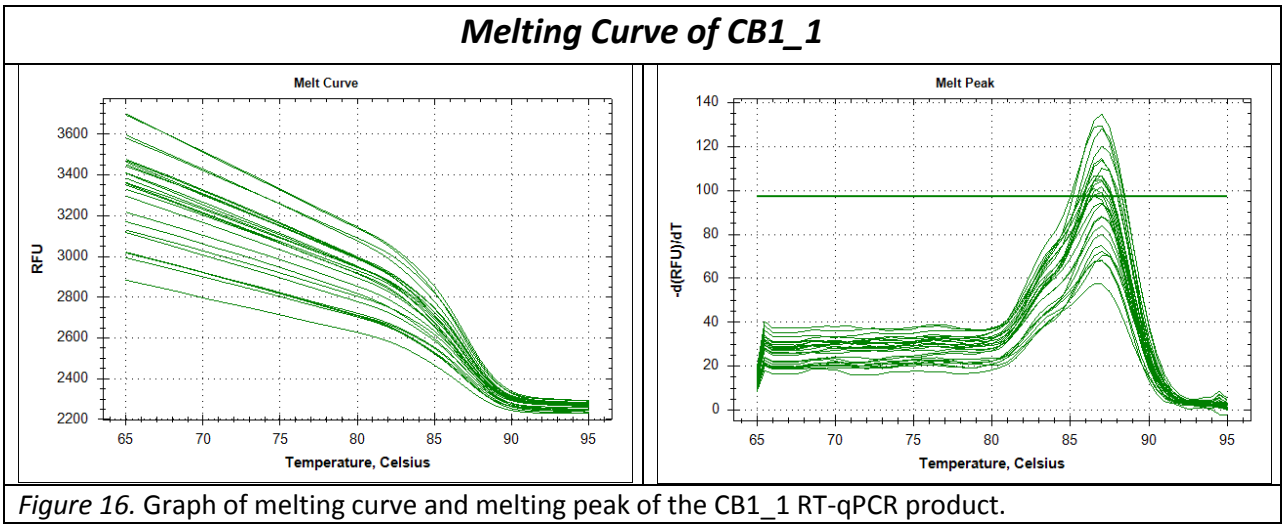

Figure 16. Graph of melting curve and melting peak of the CB1_1 RT-qPCR product.

Figure 16 shows that the RT-qPCR product of the CB1_1 primer has a melting point at about 87°C, with a wider curve than seen in Figure 14.

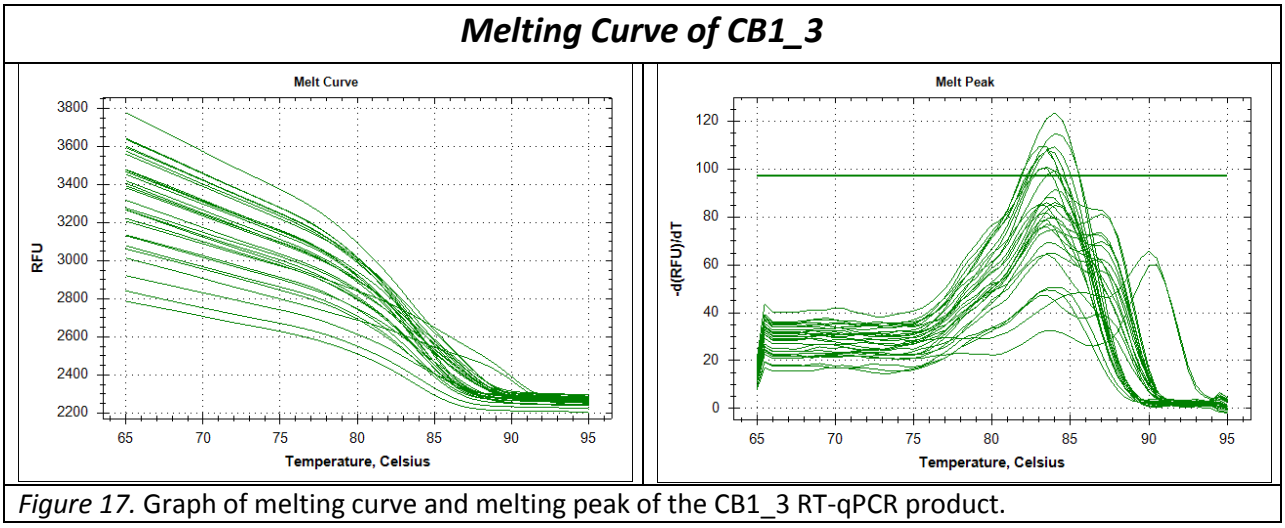

Figure 17. Graph of melting curve and melting peak of the CB1_3 RT-qPCR product.

Figure 17 shows that the melting points of RT-qPCR product for CB1_3 varied greatly with their peaks varying from 80°C to 92°C.

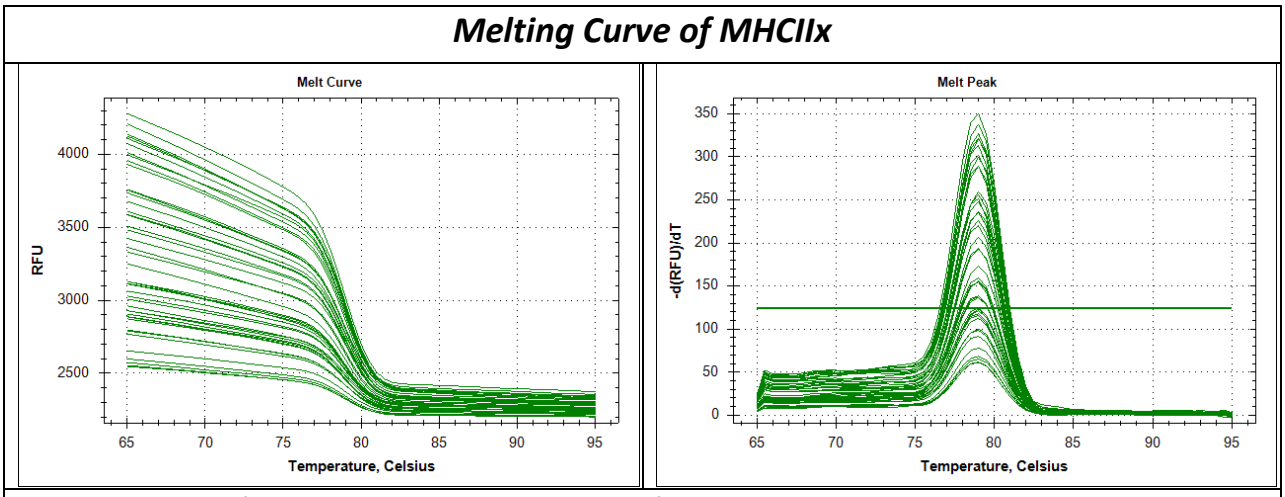

Figure 18. Graph of melting curve and melting peak of the MHCIIx RT-qPCR product.

Figure 18 shows that all the RT-qPCR product using the MHCIIx primer had the same melting point at about 79°C.

RT-qPCR Analysis using Cq values

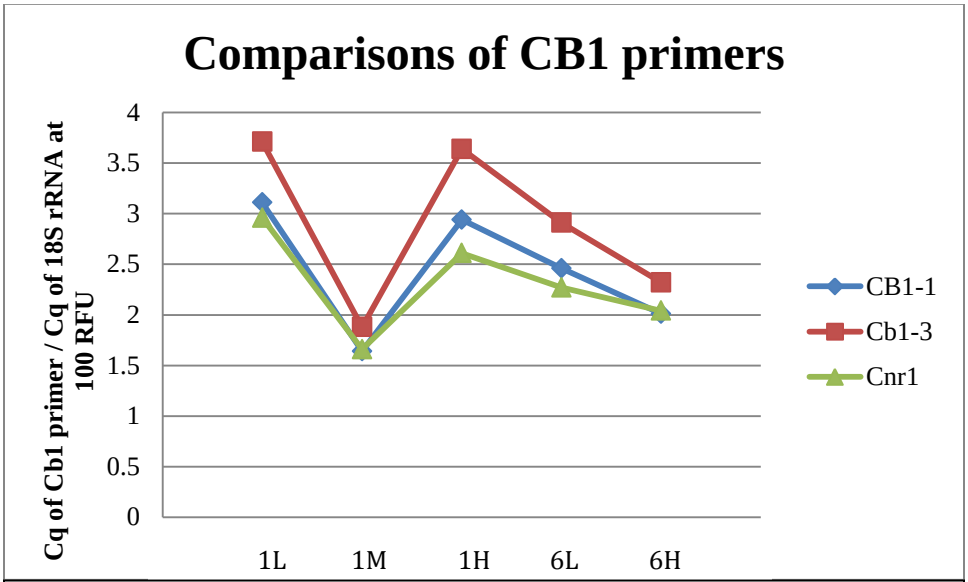

Figure 19. Graph of the Cq values (standardized with 18S rRNA Cq values) of the three CB1R primers in the five samples.

Figure 19 shows that all three primers showed the same pattern of CB1R gene expression. The highest Cq values were in the 1L and 1H samples, with the lowest being the 1M sample. The Cq value of 6L was slightly higher than the Cq value of the 6H sample. The higher the Cq value, the lower the gene expression.

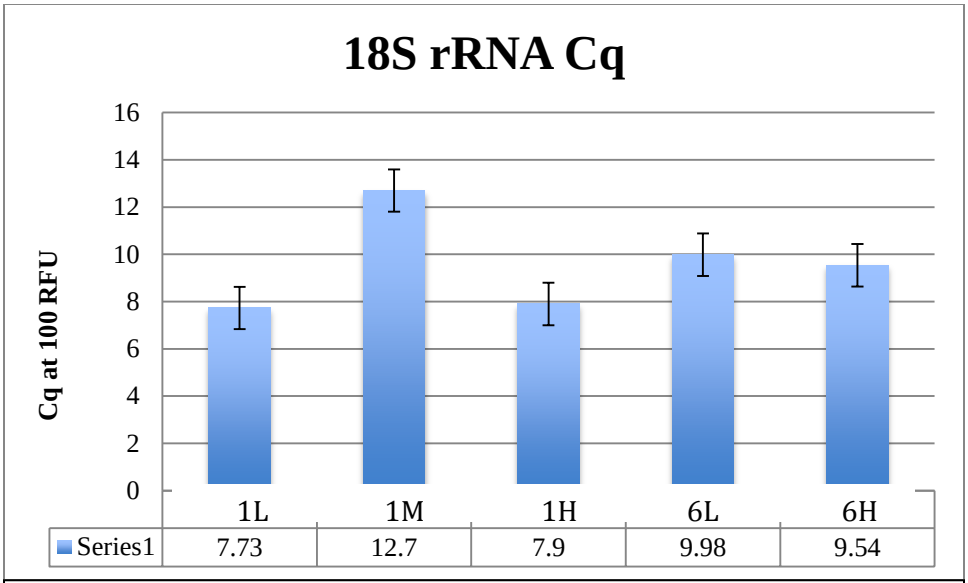

Figure 20. Graph of the Cq values (y-axis) of 18S rRNA at 100 RFU for the five samples (x-axis).

Figure 20 shows that the 1M sample took 12.7 cycles to reach 100 RFU threshold. The 1L and 1H samples were very similar and reached the 100 RFU threshold in 7.73 and 7.9 cycles, respectively. The 6L and 6H samples were also very similar and reached the 100 RFU threshold in 9.98 and 9.54 cycles, respectively.

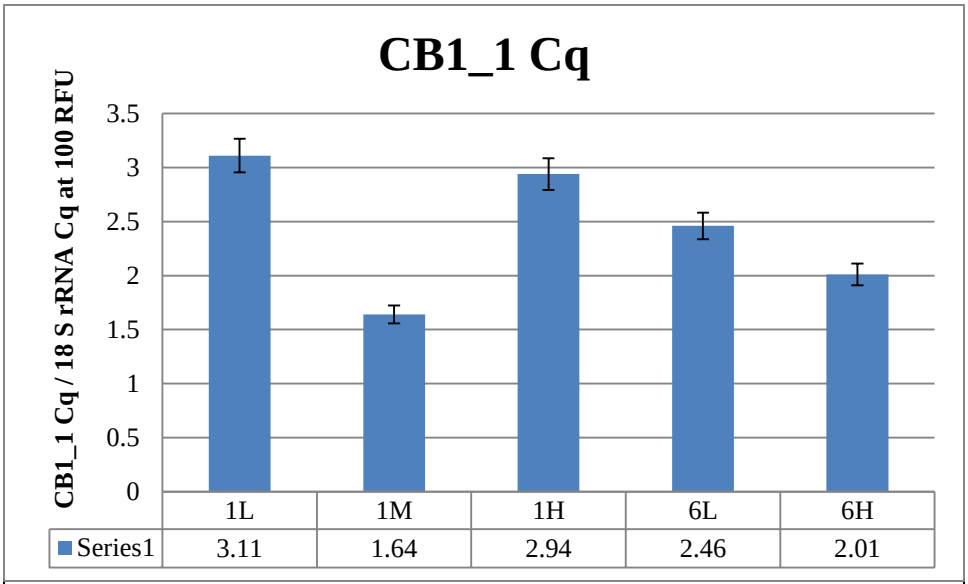

Figure 21. Graph of the Cq values (standardized with 18S rRNA Cq values) of of CB1_1 at 100 RFU for the five samples (x-axis).

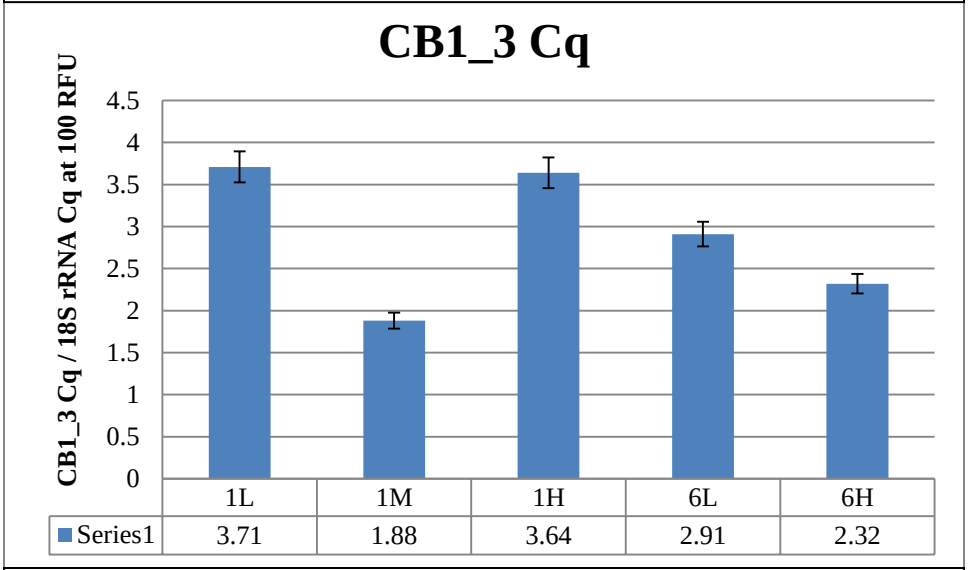

Figure 22. Graph of the Cq values (standardized with 18S rRNA Cq values) of of CB1_3 at 100 RFU for the five samples (x-axis).

Figure 21 and 22 show that the highest Cq values were seen in the 1L and 1H samples, and the lowest Cq value was seen in the 1M sample. The 6L Cq value was higher than the 6H Cq value using both the CB1_1 primer and the CB1_3 primer.

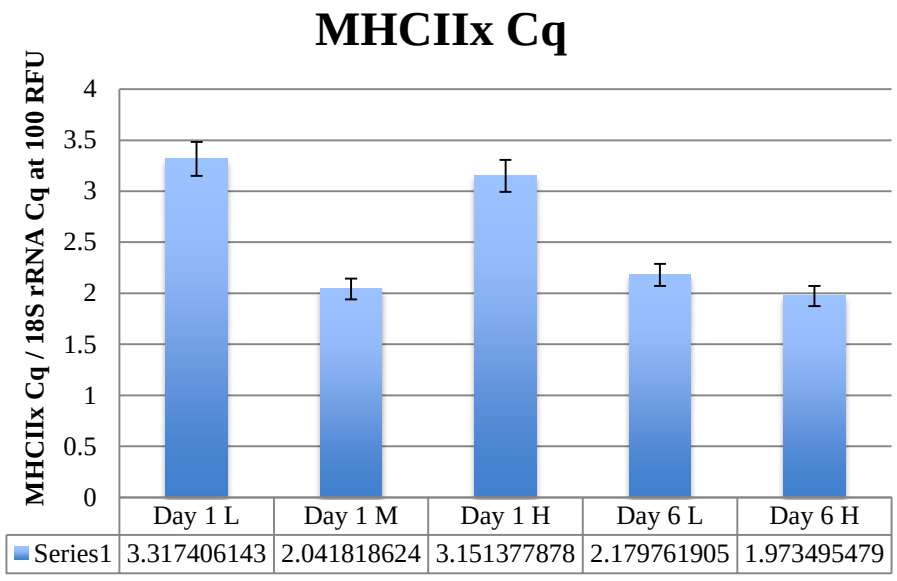

Figure 23. Graph of the Cq values (standardized with 18S rRNA Cq values) of of MHCIIx at 100 RFU for the five samples (x-axis).

Figure 23 shows that the highest Cq values were seen in the 1L and 1H samples, and the lowest Cq value was seen in the 6H sample. The 1M, 6L, and 6H samples were very similar to each other with a Cq value varying from 1.97 to 2.18.

Work Cited

American Diabetes Association. (2013). Standards of Medical Care in Diabetes – 2013. *Diabetes Care* 36, S11-S66.

Brownlee, M. (2001). Biochemistry and molecular cell biology of diabetic complications. *Nature* 414: 813-820.

Bustin, S., Benes, V., Garson, J., Hellemans, J., Huggett, J., Kubista, M., Mueller, P., Nolan, T., Pfaffl, M., Shipley, G., Vandesompele, J., Wittwer, C. (2009). The MIQE Guidelines: Minimum Information for Publication of Quantitative Real-Time PCR Experiments. *Clinical Chemistry* 55(4), 1-12.

Crespillo, A., Suárez, J., Bermúdez-Silva, F., Rivera, P., Vida, M., Alonso, M., Palomino, A., Lucena, M., Serrano, A., Pérez-Martín, M., Macias, M., Fernández-Llébrez, P., Rodríguez de Fonseca, F. (2011). Expression of the cannabinoid system in muscle: effects of a high-fat diet and CB1 receptor blockade. *Biochem. J.* 433, 175-185.

Girgenrath, S., Song, K. (2004). Loss of myostatin expression alters fiber-type distribution and expression of myosin heavy chain isoforms in slow- and fast-type skeletal muscle. *Muscle & Nerve* 31, 34-40.

Jing, H., Watkins, S., Kelley, D. (2001). Skeletal Muscle Lipid Content and Oxidative Enzyme Activity in Relation to Muscle Fiber Type in Type 2 Diabetes and Obesity. *American Diabetes Association* 50(4): 817-823.

Kim, S., Woolcott, O., Hsu, I., Stefanoski, D., Harrison, N., Zheng, D., Lottati, M., Kolka, C., Catalano, K., Chiu, J., Kabir, M., Ionut, V., Bergman, R., Richey, J. (2012). CB1 antagonism restores hepatic insulin sensitivity without normalization of adiposity in diet-induced obese dogs. *Am J Physiol Endocrinal Metab* 302, E1261-E1268.

Lanoix, D., Lacasse, A., St-Pierre, J., Taylor, S., Wthier-Chiasson, M., Lafond, J., Vaillancourt, C. (2012). Quantitative PCR pitfalls: the case of the human placenta. *Molecular Biotechnology* 52(3), 234-243.

Life Technologies. (2012). Real Time PCR Handbook.

Oberbach, A., Bossenz, Y., Lehmann, S., Niebauer, J., Adams, V., Paschke, R., Schön, MR., Bluher, M., Punkt, K. (2006). Altered fiber distribution and fiber-specific glycolytic and oxidative enzyme activity in skeletal muscle of patients with type 2 diabetes. *Diabetes Care* 29, 895-900.

Pette, D., Staron, RS. (1997). Mammalian skeletal muscle fiber type transitions. *Int Rev Cytol* 170, 143-223.

Scheen, A. (2007). Cannabinoid-1 receptor antagonists in type-2 diabetes. Best Practice & *Research Clinical Endocrinology & Metabolism* 21(4), 535-553.

Scott, W., Stevens, J., Binder-Macleod, SA. (2001). Human skeletal muscle fiber type classifications. *Physical Therapy* 81, 1810-1816.

Selvey, S., Thompson, E., Matthaei, K., Lea, R., Irving, M., Griffiths, L. (2001). Beta-actin—and unsuitable internal control for RT-PCR. *Mol Cell Probes* 15(5), 307-311.

Suresh, K., Tellabati, M., Nelli, R., White, G., Perez, B., Sebastian, S., Slomka, M., Brookes, S., Brown, I., Dunham, S., Chang, K. (2012). 18S rRNA is a reliable normalisation gene for real time PCR based on influenza virus infected cells. *Virol J* 9: 230.

Taylor, S., Wakem, M., Dijkman, G., Alsarraj, M., Nguyen, M. (2010). A practical approach to RT-qPCR- Publishing data that conform to the MIQE Guidelines. *Bio-Rad tech note 5859*.

Thorburn, A. Gumbiner, B. Bulacan, F., Wallace, P., Henry, R. (1990). Intracellular Glucose Oxidation and Glycogen Synthase Activity Are Reduced in Non-insulin-dependent (Type II) Diabetes Independent of Impaired Glucose Uptake. *The Journal of Clinical Investigation, Inc.* 85:522-529.

Zhao, D., Pond, A., Watkins, B., Gerrard, D., Wen, Y., Kuagn, A., Hannon, K. (2010). Peripheral endocannabinoids regulate skeletal muscle development and maintenance. *European Journal Translational Myology* 1(4), 167-179